Research Article

Windhu Griyasti Suci*, Harry Kasuma (Kiwi) Aliwarga, Yazid Rijal Azinuddin, Rosana Budi Setyawati, Khikmah Nur Rikhy Stulasti and Agus Purwanto

Review of various sulfide electrolyte types for solid-state lithium-ion batteries

https://doi.org/10.1515/eng-2022-0043 received October 23, 2021; accepted April 20, 2022

Abstract: The high sulfide ion polarization is known to cause increased ionic conductivity in the solid sulfidetype electrolytes. Three groups of sulfide-based solidstate electrolytes, namely, Li-P-S, Li₆PS₅X (X: Cl, Br, and I), and $Li_xMP_xS_x$ (M: Sn, Si, and Al) were reviewed systematically from several aspects, such as conductivity, stability, and crystal structure. The advantages and disadvantages of each electrolyte were briefly considered and compared. The method of the preparation was presented with experimental and theoretical studies. The analysis that has been carried out showed that the solid electrolyte Li₁₀GeP₂S₁₂ is superior to others with an ionic conductivity of 12×10^{-2} S cm⁻¹. This conductivity is comparable to that of conventional liquid electrolytes. However, the availability and high price of Ge are the problems encountered. Furthermore, because sulfide-based solid electrolytes have low chemical stability in ambient humidity, their handling is restricted to inert gas environments. When solid sulfide electrolytes are hydrolyzed, structural changes occur and H₂S gas is produced. The review's objective includes presenting a complete knowledge of sulfide-solid electrolyte synthesis method, characteristics, such as conductivity, structure, and stability, as well as generating more efficient and targeted research in enhancing the performance of the chemical substance.

Keywords: all solid-state battery, solid-state electrolyte, sulfide-type solid electrolyte

1 Introduction

The electrochemical energy storage device, such as rechargeable batteries with high power density and high energy are indispensable in their application to electric vehicles and portable electronic equipment [1]. Batteries are being extensively examined, in order to have sufficient capacity to be applied to electric vehicles. A lithium-ion (Li-ion) battery is one among the most popular commercial types as a source of electrochemical energy [2]. Li-ion batteries are superior to conventional types such as lead-acid and NiMH batteries, due to their high energy density and voltage. Li-ion battery was first coined in the 1960s and was invented in 1991 by the Sony company as an energy store in cell phones, notebook computers, and more recently for electric vehicles [3]. Liquid electrolyte is one of the most important components used in the construction of commercial lithium-ion batteries, such as lithium salt hexafluorophosphate (LiPF₆) [4]. The liquid electrolytes in Li-ion batteries are less safe when used, especially at extreme temperatures, which can trigger an explosion. Complex chemical reactions occur triggered by the presence of high temperature and voltage in Li-ion batteries [5].

High energy density and power requirements can trigger complex reactions in Li-ion batteries that are harmful to users [6]. Lithium all-solid battery (ASSLB) is a solution to the Li-ion battery problem because ASSLB has higher stability and safety than Li-ion batteries [7]. The topic of ASSLB was less attractive in its development 30 years ago because researchers considered its ionic conductivity to be relatively lower than that of solid electrolytes [8,9]. However, in the last 10 years, tremendous progress has been achieved in enhancing the ionic conductivity of solid electrolytes. The development of

Harry Kasuma (Kiwi) Aliwarga: UMG Idealab, Jakarta, Indonesia Yazid Rijal Azinuddin, Khikmah Nur Rikhy Stulasti: Material and Cell Fabrication Division, Centre of Excellence for Electrical Energy Storage Technology, Universitas Sebelas Maret, Surakarta 57146, Central Java, Indonesia

Rosana Budi Setyawati, Agus Purwanto: Department of Chemical Engineering, Faculty of Engineering, Universitas Sebelas Maret, Surakarta 57126, Central Java, Indonesia; Material and Cell Fabrication Division, Centre of Excellence for Electrical Energy Storage Technology, Universitas Sebelas Maret, Surakarta 57146, Central Java, Indonesia

^{*} Corresponding author: Windhu Griyasti Suci, Vocational School, Universitas Sebelas Maret, Surakarta 57126, Central Java, Indonesia; Material and Cell Fabrication Division, Centre of Excellence for Electrical Energy Storage Technology, Universitas Sebelas Maret, Surakarta 57146, Central Java, Indonesia, e-mail: windhugriya@staff.uns.ac.id

sulfide-based solid electrolytes with an ionic conductivity value of $2.5 \times 10^{-2} \, \text{S cm}^{-1}$, which is superior to that of liquid electrolytes, has been described [10,11].

ASSLB is depicted in Figure 1 below. A solid-state battery is composed of an anode and a cathode as negative and positive poles, respectively, as well as a solid electrolyte. This is different from Li-ion batteries which use a liquid electrolyte [12,13]. Solid-state electrolytes (SSEs) are used to replace liquid types. Li-ion media is used as a separator in traditional batteries, for deflection between the anode and cathode poles, and to prevent short circuits and electron conduction [14]. Mechanical contact is made by applying pressure to a solid-state battery array consisting of a lithium metal anode, a solid electrolyte, and a composite cathode. The SSE must have a large electrochemical stability window and high ionic conductivity [15].

SSEs are divided into three categories, they are oxides, phosphates, and sulfides. The superior SSE that are commonly

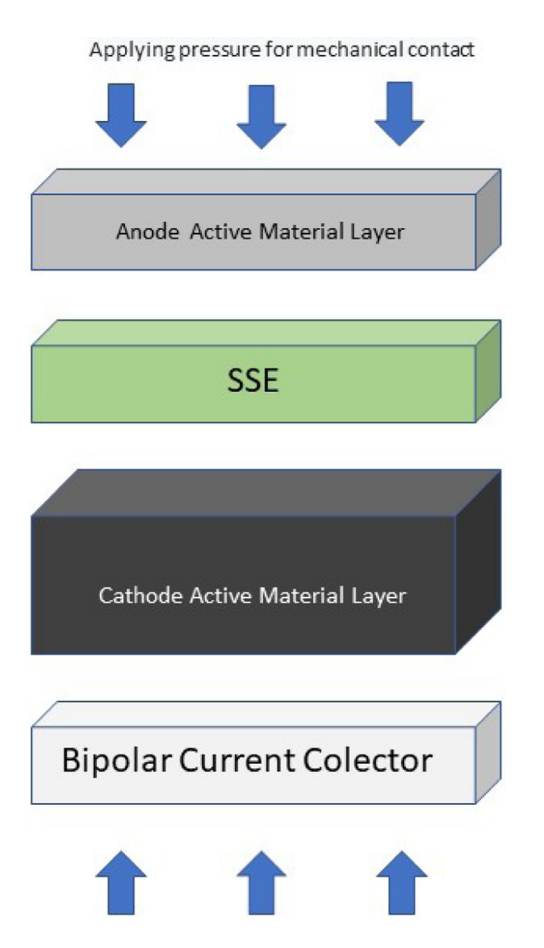


Figure 1: Arrangement of the components of a solid-state battery in which the cathode consists of a material containing an electrolyte. Composite cathodes are used to create ion pathways that are useful for increasing the voltage.

used and cover these three categories include phosphate-type Lithium Aluminum Titanium Phosphate (LATP), Lithium Lanthanum Zirconium Oxide (LLZO) oxide type, and Lithium Germanium Phosphorus Sulfide (LGPS) sulfide type. LATP has the advantage that the price of raw materials and production costs are low with the value of ionic conductivity being 0.7 mS cm⁻¹ [16,17]. Although the LATP ionic conductivity value is quite high, it is not suitable for low potential anode materials, such as lithium. This is due to a reduction in Ti⁴⁺ ions at a voltage of 2.5 V against Li/Li⁺, allowing for a short circuit in the battery [18]. LLZO (oxide type) is another category with an ionic conductivity value of 0.774 mS cm⁻¹. LLZO ionic conductivity value can still be increased with Gadoping which causes the ionic conductivity value to be 2.06 mS cm⁻¹ [19.20]. However, several challenges must be resolved before LLZO can be used in practical applications. At room temperature, LLZO reacts with ambient H2O and CO₂, lowering the ionic conductivity. Therefore, an inert atmosphere or adding additives is required in the production process. In addition, LLZO has high rigidity, as a result of its high interfacial resistance, unstable solid electrolyte, and electrode interface contact. These variables have a major influence on the cycle stability and chargeability of the battery [20]. The last category is a sulfide-based SSEs. LGPS is a sulfide electrolyte that is one of the most widely utilized SSEs. The ionic conductivity of LGPS is very high, reaching 10⁻² S cm⁻¹ at a temperature of 50–80°C [10]. Sulfide-type electrolyte is one of the materials that is considered ideal for use in solid-state batteries. Several other types of sulfide-based SSEs are depicted in the schematic diagram below.

Sulfide-type SSEs that have been successfully synthesized include Li-P-S, Li₆PS₅X (X: Cl, Br, and I), and Li_xMP_xS_x (M: Ge, Sn, Si, and Al) bases. A schematic diagram of a sulfide type SSE investigation is shown in Figure 2. The investigation began in 2005 when LPS batteries were first successfully synthesized. Furthermore, research is continued on new materials that have higher ionic conductivity. In 2008, research on Li₆PS₅X (X: Cl, Br, and I) was just started, and in 2011 research on Li_xMP_xS_x (M: Ge, Sn, Si, and Al) was started and is still ongoing. Various kinds of research were carried out because solid-state batteries still have weaknesses and challenges such as poor chemical compatibility with electrodes, narrow electrochemical stability windows, and poor mechanical properties must also be considered. The discussion in this article will focus on sulfide-based solid electrolytes. We begin with the different categories of sulfide-based solid electrolytes, their electrochemical properties, the synthesis methods used, and the material structure of each type of sulfidebased solid electrolyte are discussed. The discussion in the

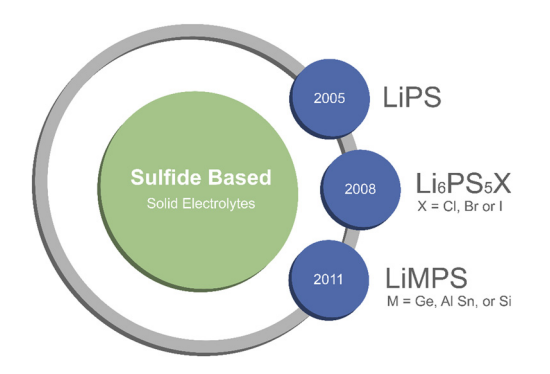


Figure 2: Schematic diagram of sulfide-based solid electrolytes.

article will end with a conclusion of perspectives and suggestions for the future improvement in sulfide-based ASSLB.

2 Sulfide-type electrolyte

Various research on solid-state batteries have been presented and one of the materials that is considered as superior to others is the sulfide. This material is known to possess excellent electrochemical properties, in the form of high conductivity and wide potential window [10,21]. Sulfide showed a high-performance solid-state lithium metal battery [22], in comparison to the conventional liquid and oxide solid electrolytes. The sulfide solid electrolytes have better mechanical characteristics [23]. Several types of sulfide solid electrolyte are LGPS and similar compounds, argyrodite (Li₆PS₅X), Li-P-S (LPS) sulfides, and their derivatives, and thio-LISICONs [24]. This section explains three groups of sulfide-based SSEs: LPS, Li_6PS_5X (X: Cl, Br, and I), and $Li_xMP_xS_x$ (M: Ge, Sn, Si, and Al).

The explanation encompass synthesis, characterization, electrochemical performance, conductivity, and the method used to determine the best sulfide-based SSE as a lithium battery application. The synthesis of sulfide solid electrolyte is generally carried out by three methods: melt quenching, ball milling, and wet-chemical [25]. Melt quenching is done by heating and suddenly lowering the temperature. Ball milling is the most common method of mechanical high-energy milling involving complex processes, including mixing and solid-state reactions. A wet chemical is a synthesis through a reaction using a solution. The structure and properties of the material are determined through characterization. Furthermore, research on the electrochemical properties of sulfide solid electrolytes, like conductivity, stability, and performance, is required to decide which sulfide based solid electrolyte is most likely to be developed.

2.1 LPS

The lithium thiophosphate or LPS class consists of several high-conducting materials. Several sulfide crystalline phases have been found, of which the type of crystal formed depends on the heat treatment applied and the composition of the glass formed. The sulfide crystalline phases include: Li_3PS_4 , $Li_7P_3S_{11}$, and $Li_4P_2S_6$ [24,26]. The composition of the glass in the LPS formed affects the ionic conductivity which relatively decreased due to the formation of individual crystals.

2.1.1 Synthesis methods

Synthetic methods that are often used in the manufacture of solid sulfide electrolytes are divided into melt quenching method, mechanical ball milling method, and wet-chemical method as illustrated in Figure 3. One of the most common methods for creating glass sulfides is the melt quenching process. The raw material mixture is sealed inside a carbon-coated quartz tube, which is subsequently heated in a furnace to a high temperature. The liquid sample was then quickly chilled using ice water. The materials experience a complex process in the mechanical ball-milling method, that includes blending, crushing, amorphization, and solid-state processes in high-energy grinding. This method offers a number of advantages, including the fact that it can be done at room temperature. Wet chemical approaches using liquid solvents as the medium are increasingly being investigated in the synthesis of solid sulfide electrolytes due to their low price, simple process, savings in time, and stability.

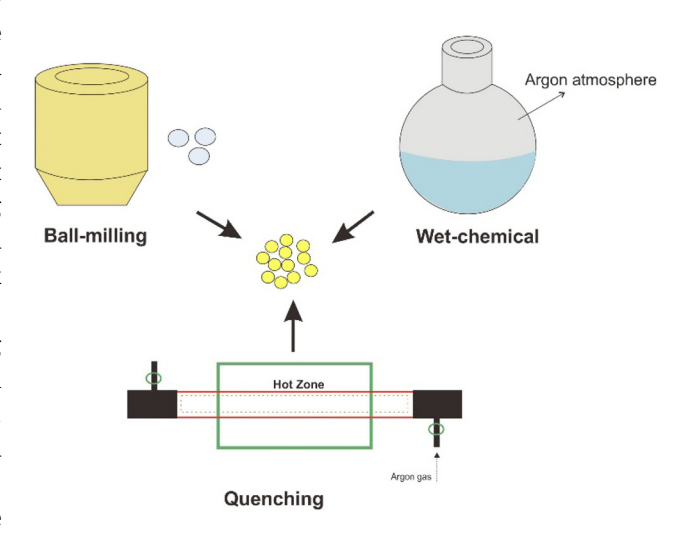


Figure 3: Synthesis methods of sulfide solid electrolyte.

In the LPS class, Li₃PS₄ is the most stable chemical. A wet chemical technique was used to make Li₃PS₄. The starting materials were Li₂S and P₂S₅ mixed in appropriate molar ratios in a glove box filled with argon (Ar), put in a quartz tube and warmed at a fixed temperature of 700°C for 8 h. After the reaction at constant temperature, the tube was cooled slowly to room temperature [27]. The synthesis using the wet chemical method was also carried out by Liu et al. on Li₃PS₄ nanopores resulting in an ionic conductivity of up to 3 times that of Li₃PS₄ crystals, which is $1.6 \times 10^{-4} \, \text{S cm}^{-1}$ [28]. In 2016, Puck et al. combined materials such as Li_2S and P_2S_5 in a $\text{Li}_2\text{S}:\text{P}_2\text{S}_5=3:1$ molar ratio with dimethyl carbonate and shook them with a zirconia ball for 5 h in a dry Ar atmosphere. The residue drying was carried out under low pressure at 90, 130, 150, and 190°C [29].

Another type of solid electrolyte in the form of LPS is Li₇P₃S₁₁. This solid electrolyte is a glass ceramic with a stable phase Li₇P₃S₁₁ which is newly formed at temperatures above 630°K [30]. The glass ceramics of Li₇P₃S₁₁ is obtained from mixing materials in the form of 70 mol% Li₂S and 30 mol% P₂S₅. For 40 h, mechanical milling was done in a planetary ball mill at 500 rpm. The whole process was performed in a glove box with H₂O below 1 ppm because the resulting material is hygroscopic. The material was then warmed at 300°C for 2h before being permitted to cool down to room temperature. After the heating process, the material is placed into a 10 mm tungsten-carbide die and then pressed with a pressure of 10 MPa [31]. Minami et al., in 2007, explored the local structure and conductivity of lithium glass Li₇P₃S₁₁ crystallized by quenching melts at various temperatures. According to their findings, P₂S₆⁴⁻ ions were formed when the melting temperature was up from 750 to 900°C [32].

The invention relating to LPS-type electrolytes with high conductivity, such as nanopores βLi₃PS₄, encourage research on Li₄P₂S₆ which is still an LPS class. The solid electrolyte Li₄P₂S₆ is known to be a product of synthesis and decomposition, obtained at high temperatures. [33, 34]. Solid electrolyte Li₄P₂S₆ is produced by mixing the basic materials in the form of Li₂S reagent level and P₂S₅ pounded using a mortar and pestle for 20 min [32, 35]. The obtained material is inserted into a quartz tube and synthesized at a high temperature. The synthesis temperature is found to be between 750 and 900°C. The powder is heated for 20 h at a temperature of 900°C and maintained for 24 h at 450°C. Anhydrous acetonitrile is used to remove the sulfur formed. After all these processes, the resulting powder was dried in a vacuum oven at 150°C for 2 h. The synthesis that occurred between 750 and 900°C produced

the same characteristics [36]. Impedance and Arrhenius measurements were carried out by applying a pressure of 300 MPa to the material to be tested, in order for the sample to form pellets with a density of $2.23 \, \mathrm{g \ cm^{-3}}$ [37,38].

2.1.2 Material characterization

The binary (100-x) Li₂S-xP₂S₅ system, as a prominent member of solid sulfide-electrolytes, is a particularly attractive electrolyte choice for solid-state batteries due to its low price, high Li-ion conductivity, and large electrochemical window compared to Li/Li⁺. Between various compositions, Li₃PS₄, Li₇P₃S₁₁, and Li₄P₂S₆ have been studied extensively because Li₃PS₄ shows good compatibility with lithium metal, Li₇P₃S₁₁ shows high electrical conductivity of greater than 10^{-3} S cm⁻¹ at room temperature, and Li₄P₂S₆ is really quite stable in preserving its structure crystals up to temperatures of 280°C in air and up to 950°C in vacuum.

Li₃PS₄ has a stoichiometry of 75% Li₂S-25% P₂S₅. The Li₃PS₄ was reported to have a y-Li₃PO₄-like structure with hexagonal closed packed sulfide ion ensembles in which the phosphorus ions are spread over the tetrahedral sites and the PS₄ tetrahedra are separated from each other [40]. In 2010, Homma et al. modified the structure of Li₃PS₄ in y, the low temperature phase, β, the middle temperature phase, and α , the high temperature phase. Figure 4 shows the arrangement of PS4 tetrahedral in the γ , β , and α phases in Li₃PS₄. The differences in the structure of y and β phases are distinguished by the location of the PS₄ tetrahedral. The arrangement of the PS₄ tetrahedral affects the position of the Li ion. The y phase shows an orderly arrangement with the top of the tetrahedral facing upwards. All of this indicates that the Li-ion is only in the tetrahedral site and the peak of the Li tetrahedral ion shows the same peak. In the β phase, the top of the tetrahedron has a zig-zag arrangement. This zig-zag arrangement causes the Li-ions to be positioned both on

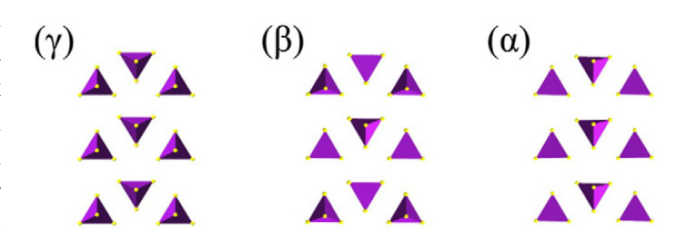


Figure 4: Arrangements of PS $_4$ tetrahedra in the γ , β , and α phase in Li $_3$ PS $_4$. Reprinted with permission from [39]. Copyright 2011, Elsevier.

the octahedral side and on the tetrahedral side, which makes the Li-ions more mobile. In phase α , the distribution of Li-ions is not clearly found [27].

Crystalline Li₇P₃S₁₁ is formed for the 70% Li₂S-30% P₂S₅ composition. The structure of Li₇P₃S₁₁ depicted in triclinic space family P-1 with a relatively large cell (V/Z = 414.7; it is 3/unit formula) made up of anions PS_4^{3-} and $P_2S_7^{4-}$ with a ratio of 1:1. Figure 5 shows the crystal structure of Li₇P₃S₁₁ glass ceramic in the triclinic centrosymmetric chamber group P-1 with 2 formula units per unit cell. All the atoms in the structure are in a common position, sharing the corners of the P₂S₇⁴⁻ ditetrahedra and PS₄³⁻ tetrahedra surrounded by Li⁺ cations [41]. The ionic conductivity of Li₇P₃S₁₁ is produced by the collective movement of many defects, not by the sluggish diffusion of isolated defects. Most Li sites are connected tetrahedral (LiS₄) and are joined by further empty tetrahedral sites (S₄). This results in a 3D diffusing path with a flat energy profile [31].

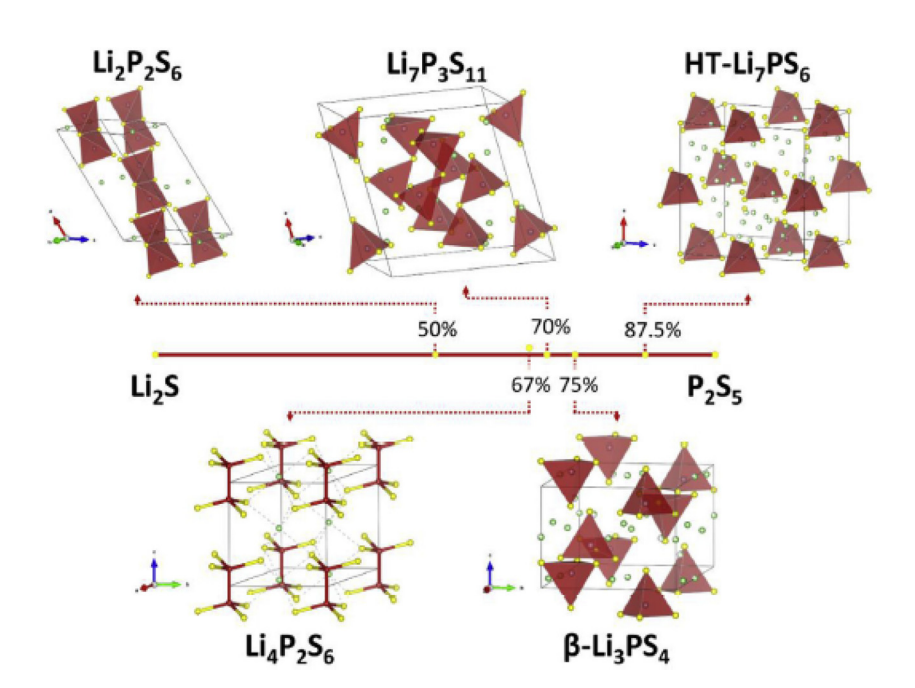
The reaction that creates $\text{Li}_4\text{P}_2\text{S}_6$ crystals is peculiar in that the composition is not perfectly positioned on the $\text{Li}_2\text{S}-\text{P}_2\text{S}_5$ bond line. This can be calculated using the 67 mol% Li_2S composition, which is applied to the $\text{Li}_4\text{P}_2\text{S}_7$ stoichiometry. $\text{P}_2\text{S}_6^{4-}$ anions are the most common building units in $\text{Li}_4\text{P}_2\text{S}_6$ crystals [36]. The structure of $\text{Li}_4\text{P}_2\text{S}_6$ in the P63/mcm space group was characterized by Mercier et al. [40]. These crystals are made up of P_2S_6 ions with D3d symmetry and P–P bonds oriented along the crystallographic axis. The crystal's basic structure

projected into a hexagonal plane. The location of all P–P bonds along the same c axis is determined by the P–P bond placement in the crystal unit. Dietrich et al. demonstrated that crystalline $\text{Li}_4\text{P}_2\text{S}_6$ could only be manufactured using a glass-ceramic microstructure with a mostly PS_4^{3-} unit amorphous component [42].

2.1.3 Electrochemical properties

Li₃PS₄ is by far the most stable chemical in the LPS class, with an activation energy of 60-73 kJ mol⁻¹ and a low ionic conductivity of 3×10^{-7} S cm⁻¹ at room temperature. The tetrahedral arrangement of PS₄ affects the position of the Li-ions. The y phase displays an organized pattern with the top of the tetrahedral side up. All this indicates that the Li-ion is only in the tetrahedral site and that the peaks of the Li tetrahedral ion show the same peak. The y phase shows an activation energy of 21.3 kJ mol⁻¹ at room temperature with an ionic conductivity of $3.0 \times 10^{-7} \,\mathrm{S\,cm^{-1}}$. While in phase β , they are arranged in a zig zag fashion, which causes the Li-ions to be positioned both on the octahedral side and on the tetrahedral side, which makes the Li-ions more mobile. The phase shows an activation energy of 15.5 kJ mol⁻¹ with a better ionic conductivity of $3.0 \times 10^{-2} \,\mathrm{S}\,\mathrm{cm}^{-1}$ at 500 K [39].

The Li_3PS_4 nanostructure possesses a large electrochemical window and is chemically stable to lithium metal (5 V). The ionic conductivity of manipulated solid



 $\textbf{Figure 5:} \ \ \text{The crystal structures of Li}_2 S_{\text{P}_2} S_{\text{5}} \ \text{binary system.} \ \ \text{Reprinted with permission from [41]. Copyright 2018, Elsevier.}$

electrolytes has far-reaching ramifications for the synthesis of materials in battery applications [28]. The lithium metal anode also functions as a coating to prevent the formation of dendrites, improves electrochemical performance, and reduces parasitic side reactions [43]. The glass-ceramic material Li₃PS₄ (with polymorph, 7.5 \times 10 $^{-4}$ S cm $^{-1}$) [44] had a substantially greater ionic conductivity at ambient temperature (room temperature, RT) than the bulk crystal material (polymorph, 9 \times 10 $^{-7}$ S cm $^{-1}$) [45]. Although the reason for the higher conductivity in glass ceramics is unknown, the nanocrystalline β Li₃PS₄ produced using wet chemical method has a respectable ionic conductivity (1.6 \times 10 $^{-4}$ S cm $^{-1}$ at ambient temperature).

In terms of ionic conduction qualities, the material's structure is crucial to the conductivity process. Due to the 3D conduction pathway generated by the crystal structure [30], the ionic conductivity of Li₇P₃S₁₁ glass increases from 8×10^{-5} to 1.4×10^{-3} S cm⁻¹ in the stoichiometric situation of 70% mol percent Li₂S - 30% mol percent P₂S₅. The cold-pressed Li₇P₃S₁₁ has an ionic conductivity of $1.3 \times 10^{-3} \, \text{mS cm}^{-1}$ [46]. The deposition of superionic crystals reflected by Li₇P₃S₁₁ [47] results in high ionic conductivity. As with other types of solid sulfide electrolytes, glass ceramics Li₇P₃S₁₁ is found to be very sensitive to air and also contributes to gas formation (such as H₂S, a poisonous gas) [48]. The electrochemical stability of Li₇P₃S₁₁ with Li metal as the anode, carrying 5 V with the activation energy (E_a) , recovered from the theoretical estimated fitting is 187 meV [49].

 $\text{Li}_4\text{P}_2\text{S}_6$ is a relatively stable thiophosphate substance, maintaining its crystal structure at temperatures as high as 280°C in air and 950°C in vacuum. Despite having a low ionic conductivity of $2.38 \times 10^{-7}\,\text{S cm}^{-1}$ at 25°C and $2.33 \times 10^{-6}\,\text{S cm}^{-1}$ at 100°C, the crystalline conductivity of $\text{Li}_4\text{P}_2\text{S}_6$ can be dramatically improved (from 2.9×10^{-11} to $10^{-6}\,\text{S cm}^{-1}$) by the addition of amorphous components at RT [42]. Similarly, despite the fact that the process of conduction is unknown, it is clear that high conductivity may be attained using a variety of designs [41]. For all materials in the LPS family, however, the high conductivity is not always generated from the crystalline phase.

2.2 Li₆PS₅X (X: Cl, Br, and I)

Lithium argyrodites $\text{Li}_6\text{PS}_5\text{X}$ (X: Cl, Br, and I) are one type of sulfide solid electrolyte that has a rather high ionic conductivity at 298 K, with values ranging from 10^{-2} to $10^{-3}\,\text{S}\,\text{cm}^{-1}$ for Br and Cl [50,51]. The addition of anions to the solid electrolyte has been shown to increase the

conductivity. The size and polarizability of the anions coordinated to the mobile cations are the most important factors that influence conductivity [40]. This section explains several types of Li-argyrodites sulfide-based solid electrolytes, such as $\text{Li}_6\text{PS}_5\text{Cl}$, $\text{Li}_6\text{PS}_5\text{Br}$, and $\text{Li}_6\text{PS}_5\text{I}$.

2.2.1 Synthesis methods

In 2008, Li₆PS₅X (X: Cl, Br, and I) crystals were successfully produced through a stoichiometric reaction involving Li₂S, P₂S₅, and LiX in an inert gas. The synthesized material was pressed and heated for 7 days at a temperature of 823 K [52]. Subsequent studies have shown that the preparation time of Li₆PS₅X can be reduced, resulting in a solid electrolyte with an argyrodite phase with an appropriate crystallinity value. In 2011, Li₆PS₅X synthesis was successfully completed through a mechanical milling method for 24 h with annealing for 5 h at a temperature of 823 K [53]. Then, Li₆PS₅X is synthesized rapidly using high energy mechanical milling and annealed at 550°C for 5 h which produces an ionic conductivity of 0.74 mS cm⁻¹ at 298 K for X = Cl and Br [54]. The annealing temperature of SSE materials greatly affects their performance and ionic conductivity [55]. It needed higher temperature treatment to reach large ionic conductivity value [56].

Milling time was shown to affect the Li-ion conductivity. The longer the grinding time, the smaller the resistance, resulting in an increase in Li-ion conductivity [55]. Therefore, the optimum milling time needs to be investigated. Due to the reactivity of the sample to moisture and oxygen in the air, all phases of solid electrolyte preparation were carried out in an Ar atmosphere.

In addition to using the solid-state method, the synthesis of $\text{Li}_6\text{PS}_5\text{X}$ can be carried out using a wet chemical method with an anhydrous tetrahydrofuran (THF) solvent. Li_2S and P_2S_5 were mixed in a mortar and then dissolved into THF, then mixed for 24 h at room temperature. Li_2S and LiX dissolved in ethanol were added to the mixture. After mixing for 24 h, the solution was centrifuged at 8,000 rpm for 10 min. The result, in the form of a clear solution, is dried and pressed, then sintered for 6 h at 550°C. All synthesis steps were completed in an Ar filled glove box [57,58].

2.2.2 Material characterization

 $\text{Li}_6\text{PS}_5\text{X}$ (X: Cl, Br, and I), or argyrodite, has a high conductivity, and it is easily fabricated [59]. $\text{Li}_6\text{PS}_5\text{X}$ is a halide-substituted from Li_7PS_6 derivative [60]. The Li_7PS_6

type and its variants, such as Li₆PS₅X, have a non-bcc type anion framework with a network of tetrahedral sites for mobile cations [11]. In the structure of Li₆PS₅X crystal, the unit cell in a completely ordered arrangement is a face centered cubic lattice of halide ions (Wyckoff 4a). PS_{4}^{3-} , which has P on the Wyckoff 4b site, fills the octahedral gaps produced by the halide ions. The Wyckoff 4d site, often known as the "free S site," and the tetrahedral site (Wyckoff 16e) are the two potential locations for S [61]. The structure of Li₆PS₅X crystal, which is depicted in Figure 6, crystallizes in the space group F43m with cubic symmetry. Li-ions only fill the 24g locations of the split site 48h-24g-48h ' in Li₆PS₅Cl. They are spread over the 24g and 48h locations in compounds with X = I and Br. PS_{μ}^{3-} tetrahedra are formed when P occupies 4b and S²⁻ occupies 16e. Unlike Li₆PS₅I, where halide anions occupy exclusively the 4a sites, Li₆PS₅Br has occupation factors of 78% (4a) and 22% (4b) according to neutron diffraction (4d). The occupation factors for Li₆PS₅Cl are 39% (4a) and 62% (4d), respectively, indicating that the bulk of Cl anions occupy the inner centers of the Li cages, which are too tiny for I [62]. The structure of Li₆PS₅X is similar to that of pure Li₇PS₆ as indicated by the XRD test showing the same peaks at 2θ , 25.5° , 30° , and 31.2° [63]. To avoid direct contact of the sample to the moisture and oxygen content of the air, XRD testing of Li₆PS₅X samples must also be completed in an Ar atmosphere [55].

2.2.3 Electrochemical properties

Deiseroth et al. found that the mobility of Li ions in $\text{Li}_6\text{PS}_5\text{X}$ reaches $10^{-2}-10^{-3}\,\text{S}\,\text{cm}^{-1}$, which approximates the mobility of Li-ions in the liquid electrolyte LiPF₆ in

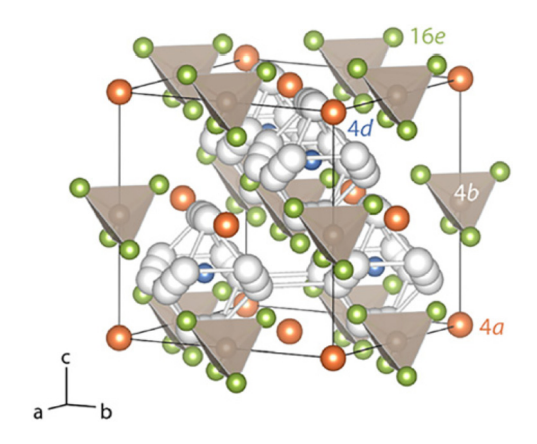


Figure 6: Li $_6$ PS $_5$ X crystal structure (X: Cl, Br, and I). The X anions form a cubic close packed lattice with PS $_4$ tetrahedra in the octahedral sites and free S 2 in half of the tetrahedral sites. Reprinted with permission from [62]. Copyright 2018, American Chemical Society.

carbonates [52]. $\text{Li}_6\text{PS}_5\text{X}$ synthesis via ball milling method produced an ionic conductivity value of $10^{-3}\,\text{S}\,\text{cm}^{-1}$ at 298 K [53]. Because of their excellent ionic conductivity at RT, these compounds are considered one of the best solid electrolytes for high-energy all-solid-state battery applications.

The maximum ionic conductivity of $\text{Li}_6\text{PS}_5\text{Cl}$ obtained by ball milling process and annealing at 250°C is 1.1 mS cm⁻¹. In 2016, Zhou et al. did the synthesis of $\text{Li}_6\text{PS}_5\text{Cl}$ with a solution-based preparative method, using THF/ethanol mixtures which resulted in a fairly large ionic conductivity value reaching 3.9 mS/cm of the formula $\text{Li}_{6-y}\text{PS}_{5-y}\text{Cl}_{1+y}$ with y=0-0.5 [57]. Besides that, preparation of the composite using liquid-involved synthesis methods is more promising [64]. All solid-state batteries with the application of the $\text{Li}_6\text{PS}_5\text{Cl}$ electrolyte using a composite cathode containing 1% by weight of ethyl cellulose has a capacity of 111.7 mA h g⁻¹ and is quite stable after 100 cycles. This shows that $\text{Li}_6\text{PS}_5\text{Cl}$ is capable enough to be used as a solid electrolyte [65].

Li₆PS₅Br has the highest ionic mobility of Li⁺ ions among others [52] with Li jump rate of $10^9 \,\mathrm{s}^{-1}$ at 298 K [51]. Synthesis of Li₆PS₅Br was successfully carried out by ball milling and annealing for 5 h at 300°C, and milling further for 4 h at 450 rpm. The ionic conductivity of Li₆PS₅Br reached 1.38 mS cm⁻¹ [55]. Li₆PS₅Br synthesized via liquid-phase method using THF and EtOH has ionic conductivity of 3.1 mS cm⁻¹ at 298 K. [66]. The ionic conductivity was enhanced by various doping methods, such as substitution [25]. Substitution to Li₆PS₅Br formula affects the structure and ionic mobility properties. The substitution of Li_6PS_5Br with formula $Li_{6.35}P_{0.65}$ $Si_{0.35}S_5Br$ result in ionic conductivity value of 2.4 mS cm⁻¹ [67]. Furthermore, substitution of S using Se in Li₆PS₅Br with formula Li₆PS_{5-x} Se_xBr results in higher ionic conductivity value of 3.9 mS cm⁻¹ [68]. Batteries with solid electrolyte Li₆PS₅Br as a mixture in the composite cathode are proven to have good performance and stability [69,70]. Li₆PS₅Br has been successfully applied to battery and managed to achieve a high and fairly stable capacity [71,72]. Therefore, the Li₆PS₅Br is capable enough to be used as SSEs [69,70].

Ionic conductivity and interfacial kinetics were also improved by the addition of I [73,74]. The I-based conductors synthesized through the solvent-based method have a total ionic conductivity value of $0.12\,\mathrm{mS}\,\mathrm{cm}^{-1}$ at 298 K and a bulk ionic conductivity of $1.3\,\mathrm{mS}\,\mathrm{cm}^{-1}$ [75] at 500 K. The ionic conductivity was enhanced by various doping methods, such as substitution. The substitution of Ge into $\mathrm{Li}_6\mathrm{PS}_5\mathrm{I}$ with the formula $\mathrm{Li}_{6.6}\mathrm{P}_{0.4}\mathrm{Ge}_{0.6}\mathrm{S}_5\mathrm{I}$ was conducted and resulting ionic conductivity value was up to $18.4\times10^{-3}~\mathrm{S}\,\mathrm{cm}^{-1}$ with further sintering. [76].

Anion doping could potentially help to improve the stability of SSEs. The high electrochemical windows are found in sulfide electrolytes containing halogen components [77]. Li₆PS₅X also has a large chemical stability window for Li-ions which reaches 7 V [78]. Cyclic voltammetry under the observed conditions of the Li₇P₂S₈I electrolyte revealed electrochemical stability of up to 10 V vs Li/Li⁺ [73]. This is high among other types of sulfide electrolytes [79, 80]. Therefore, with its high electrochemical stability and excellent value of ionic conductivity, Li₆PS₅X is acceptable to be used as a solid electrolyte in the Li-ion batteries [81].

2.3 $Li_xMP_xS_x$ (M: Ge, Sn, Si, and Al)

Li_xMP_xS_x is a derivative of the ceramic thio-LISICON group, a group of solid electrolytes with good characteristics. $Li_xMP_xS_x$ is a derivative form of L-P-S system. $\text{Li}_{10}\text{GeP}_2\text{S}_{12}$ (LGPS) is the first $\text{Li}_x\text{MP}_x\text{S}_x$ group developed, which is the result of the development of the LiS-PS form of the system, which was detected to have Li₃PS₄ and Li₄GeS₄ structures [82]. Ceramic-sulfide solids, such as Li₁₀GeP₂S₁₂ (LGPS), have gotten a lot of interest because of their high ionic conductivity of 1–25 mS cm⁻¹ [83]. The presence of Ge in Li₁₀GeP₂S₁₂ have disadvantages in terms of availability and cost of materials. However, there are several alternatives that change the Ge component in $Li_{10}GeP_2S_{12}$. LGPS has a chemical formula ($Li_xMP_xS_x$), where M represents Ge which is replaceable with M: Sn, Si, and Al. Li₁₀GeP₂S₁₂ (LGPS) has been examined further and shows very high ionic conductivity values. However, the price of Ge is quite high, and its limited availability means that other alternatives are needed in order to be manufactured at lower prices [49]. Some alternatives that are used include Sn, Si, or Al because they maintain a similar polygon structure [31]. This section explains several types of sulfide-based solid electrolytes, such as $Li_{10}GeP_2S_{12}$, $Li_{10}SnP_2S_{12}$, $Li_{10}SiP_2S_{12}$, as well as $Li_{11}AlP_2S_{12}$.

2.3.1 Synthesis methods

The synthesis of $\text{Li}_{10}\text{GeP}_2\text{S}_{12}$ was carried out by mixing starting materials, such as germanium sulfide (GeS₂), lithium sulfide (Li₂S), and phosphorus sulfide (P₂S₅) in a 5:1:1 molar ratio with agate mortar. The heat was given during the mixing process [84]. The sample is formed into pellets by applying pressure for the thickness to become 1 mm. The crystallization phase of $\text{Li}_{10}\text{GeP}_2\text{S}_{12}$ is carried

out by synthesis at above 400°C [85]. The material sintering process is carried out for 8 h at 700°C. The sintered material tends to be in the form of lumps of samples that need to be pulverized into powder for further processing [86]. The $\text{Li}_{10}\text{GeP}_2\text{S}_{12}$ was synthesized using a solid-state method and carried out in glove boxes at an Ar atmosphere, because the material is very sensitive to moisture and to avoid the formation of H_2S [84].

A series of investigations of glassy solid electrolytes, such as $\text{Li}_{11}\text{AlP}_2\text{S}_{12}$ have been carried out previously with Al^{3+} replacing Ge^{4+} in $\text{Li}_{10}\text{GeP}_2\text{S}_{12}$ and presenting high Li. Al^{3+} substitution was identified to remove non-bridging sulfur which limits the conduction of Li-ions [63]. The synthesis of $\text{Li}_{11}\text{AlP}_2\text{S}_{12}$ was carried out by mixing Al_2S_3 , P_2S_5 , and Li_2S . The molar ratio of each ingredient is 11:2:1. The mixing is carried out mechanically by ball milling for 10 h with a speed setting of 350 rpm. As a result of sintering mixing, the material is inserted into a glass tube. The sintering was carried out at various temperatures of 400, 500, and 600°C for 18 h. The synthetic variations were denoted by LAlPS400, LAlPS500, and LAlPS600 [87].

Synthesis using Si and Al is a problem because it is difficult to achieve the desired polygon structure. From the three alternatives for replacing Ge, the use of Sn is preferable. $\text{Li}_{10}\text{SnP}_2\text{S}_{12}$ (LSnPS) was synthesized by mixing P_2S_5 , Li_2S , and nanocrystal SnS_2 which had been synthesized before in a molar ratio of 5:1:1. This mixture was ball milled at 600 rpm for 30 min. Then, sintered with a vacuum quartz tube for 2 h at 500, 550, 600, and 650°C, and then cooled. All of the processes for preparing LSnPS should be performed in dry Ar gas atmosphere glove box which contains O_2 and H_2O under 1 ppm [33].

 $\text{Li}_{10} \text{SiP}_2 \text{S}_{12}$ (LSiPS) was synthesized by mixing up $\text{P}_2 \text{S}_5$, $\text{Li}_2 \text{S}$, and SiS_2 with a molar ratio of 5:1:1, using ball milling for 20 h at 500 rpm in a 500 mL stainless steel tube. The powder was pressed to form pellets on a 375 MPa Ti-die with a diameter of 1.3 cm to a thickness of 2 mm. The pellets were heated for 8 h at 550°C and then crushed with a mortar and pestle.

Solid-state sulfide-based batteries are assembled to facilitate an Ar atmosphere. Besides, the challenge in using sulfide materials as SSE is the formation of H_2S which should be prevented by the use of metal sulfide and metal oxide additives [88].

2.3.2 Material characterization

Analysis of the structure of the Li₁₀GeP₂S₁₂ material has been reported previously. The structure is shown in the

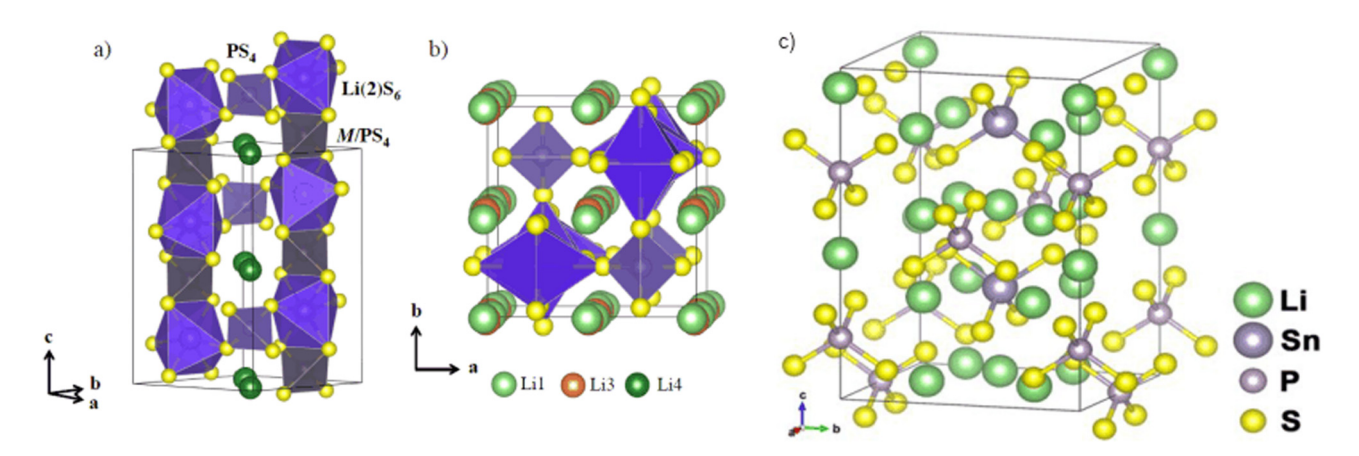
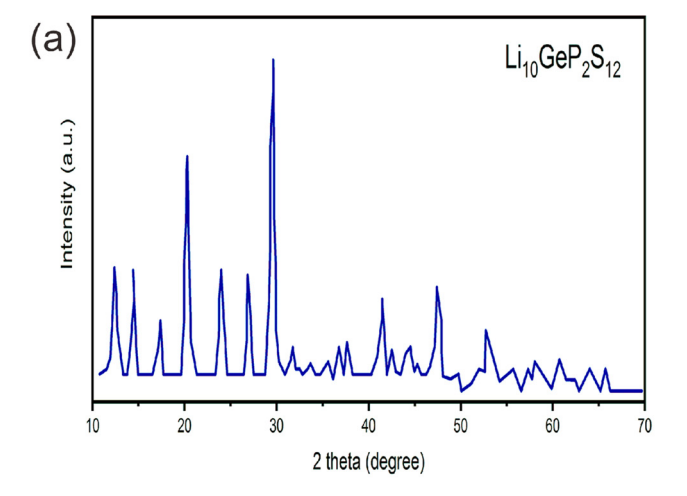


Figure 7: Crystal structure of $Li_{10}GeP_2S_{12}$ (a and b). (a) Chains of $(Ge/P)S_4$ tetrahedral and Li_2S_6 octahedral with shared edges formed a rigid structural framework in which chains are connected in the <110> direction by the PS₄ tetrahedra. (b) The structural framework as a polyhedral representation in the <001> direction. Reprinted with permission from [90]. Copyright 2016, American Chemical Society. (c) Structure of $Li_{10}SnP_2S_{12}$. Reprinted with permission from [95]. Copyright 2019, American Chemical Society.

Figure 7(a) and (b). The structure of $\text{Li}_{10}\text{GeP}_2\text{S}_{12}$ is a 3D framework composed of LiS_4 tetrahedral, $(\text{Ge}_{0,5}\text{P}_{0,5})\text{S}_4$ tetrahedral, LiS_6 octahedral, and PS_4 tetrahedral [10], [89]. The structure is made up of an immobile framework of PS_4 and $(\text{Ge/P})\text{S}_4$ tetrahedral, as well as a possibly immobile octahedral LiS_6 complex. The average bond length for Li-S bond is 2.65, which is a respectable length. As a result, the LiS_6 octahedron (also known as the Li_2 site) has been included in the framework. The $(\text{Ge/P})\text{S}_4$ tetrahedral shared edges with the LiS_6 octahedral, creating chains in the <001> direction that are linked by PS_4 tetrahedral along the <110> location. Besides, the transport of Li-ions and the high conductivity of LGPS have been attributed to a 1D diffusion channel using two Li-locations (Li_1 and Li_3 , respectively) along the <001> direction, in

between the chains produced by (Ge/P)S₄ tetrahedral [90]. The analysis test using XRD on the Li₁₀GeP₂S₁₂ material is shown in the Figure 8(a) which shows the typical spectral features of early P₂S₅, GeS₂, and Li₂S materials, while the band peaking at around 495 cm⁻¹ was detected as Li₁₀GeP₂S₁₂ material [91]. The main characteristic of the diffraction peak is at $2\theta = 20^{\circ}$, 26.7°, and 29.4° for Li₁₀GeP₂S₁₂, corresponding to a tetragonal of the *P*42/*nmc* space group [92]. The crystallite with a size of 723.21 Å has a high purity with an electrolyte impurity of less than 3.

The characterization test of $\text{Li}_{11}\text{AlP}_2\text{S}_{12}$ in the form of X-ray diffraction (XRD) analysis has been carried out and from the analysis results, the $\text{Li}_{11}\text{AlP}_2\text{S}_{12}$ shows peaks and characterization similar to $\text{Li}_{10}\text{GeP}_2\text{S}_{12}$ [93]. The crystal



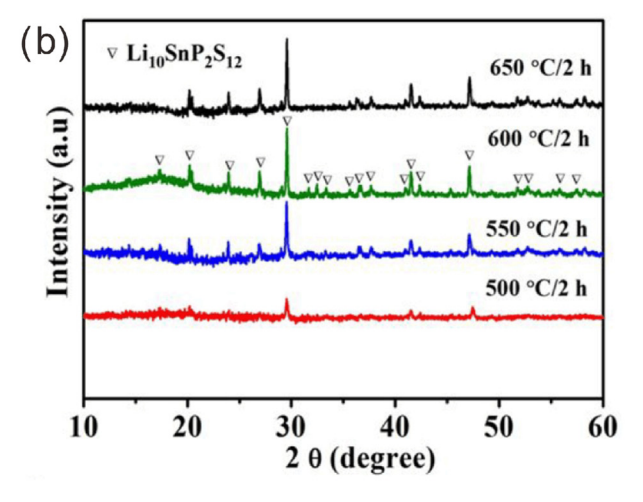


Figure 8: (a) X ray diffraction of the Li₁₀GeP₂S₁₂ solid electrolyte. Reprinted with permission from [91]. Copyright 2013, Elsevier. (b) XRD pattern of Li₁₀SnP₂S₁₂ at various annealing temperatures. Reprinted with permission from [95]. Copyright 2019, American Chemical Society.

structure of $\text{Li}_{11}\text{AlP}_2\text{S}_{12}$ is typical 3D thio-LISICON which has the arrangement of (Al/P) tetrahedral or and forms a 3D chain structure because it is connected by LiS_4 tetrahedral and LiS_6 octahedral [87].

Li₁₀SnP₂S₁₂ (LSnPS) structure is a polygon crystal with a space group of P42/mc a = 8.854 Å, and c =12.851 Å lattice parameters. The 3D percolating structure shows that ion conductivity Li⁺ is high [47]. Li₁₀SnP₂S₁₂ structure is seen in Figure 7(c). The Li₁₀SnP₂S₁₂ crystal structure was characterized by XRD. The XRD pattern shown in Figure 8 indicates comparison between annealing temperatures of 500, 550, 600, and 650°C. The diffraction peaks corresponding to the $Li_{10}SnP_2S_{12}$ crystalline phase increased at 29.3°, 41.3°, 47.1° and 500°C strong temperature. The top of diffraction which are recognized as the crystalline phase of Li₁₀SnP₂S₁₂ formed approximately at 20.1°, 23.8°, 26.7°, 36.2°, and 37.3° of the sample at the annealing temperature of 550°C. The multiple peak crystallization is identified and the strength of the XRD pattern is boosted greatly at 600°C as the optimum strong temperature. This indicates that the Li₁₀SnP₂S₁₂ has a high crystallization, which improves the electrolyte's ionic conductivity significantly. However, following strong temperature at 650°C, the diffraction peaks at 17.1°, 34.2°, 34.5°, and 34.8° of the Li₁₀SnP₂S₁₂ disappeared. These results showed that the best annealing temperature to synthesize LSnPS is at 600°C. The LSnPS powder particles measure up to 1-3 µm and the diameter of LSnPS pellet is 10 mm and the thickness is 1.1 mm [33]. To measure crystallization level of the final LSiPS material, an XRD analysis was performed. The resulting XRD pattern shows the structural similarity between LSiPS and LGPS. Based on the crystal structure, LGPS and LSiPS have the same structure in the space group of P42/mc (no. 137) with a lower lattice parameter value than $\text{Li}_{10}\text{GeP}_2\text{S}_{12}$ (LGPS), a = 8.6512 (5) Å and c = 12.5095 (8) Å as demonstrated by Le Bail refinements [94]. Interestingly, LSiPS and LGPS have a near identical structure. According to the Rietveld, the LSiPS and LGPS structures have a secondary phase of approximately 15% LISICON. This phase reduces the high level of pure superionic polygon conductivity. This is due to the fact that LGPS and LSiPS are extremely sensitive to heat and environmental conditions.

2.3.3 Electrochemical properties

SSEs $\rm Li_{10}GeP_2S_{12}$ (LGPS) is a type of sulfide with a high conductivity value at 298 K. Ionic conductivity of $\rm Li_{10}GeP_2S_{12}$ can be compared to liquid organic electrolytes in Li-ion. The $\rm Li_{10}GeP_2S_{12}$ is expected to have a high solid-state battery

charge and discharge performance because it has high ionic conductivity [82]. The $\text{Li}_{10}\text{GeP}_2\text{S}_{12}$ (LGPS) is an interesting material after the first discovery in 2011, which showed ionic conductivity value of $12\,\text{mS}\,\text{cm}^{-1}$ at 298 K [10]. This value is obtained from the sum of bulk resistance and grain boundaries. The temperatures between 100 and 110°C show activated energy of 24 kJ mol⁻¹ which identifies it as a super ionic conductor [10].

 ${\rm Li_{11}AlP_2S_{12}}$ has ionic conductivity value of 0.802 mS cm⁻¹ at 298 K, and has electrochemical stability up to 5.0 V with an activation energy of 25.4 kJ mol⁻¹. The Li-ion conduction in ${\rm Li_{11}AlP_2S_{12}}$ has potential and important in solid-state battery development [87].

The synthesis of $\text{Li}_{10}\text{SnP}_2\text{S}_{12}$ (LSnPS) has total ionic conductivity value of $3.2\,\text{mS}\,\text{cm}^{-1}$ at $300\,\text{K}$. Meanwhile, the instability of $\text{Li}_{10}\text{SnP}_2\text{S}_{12}$ electrolyte in the lithium anode becomes one of the disadvantages. However, no obvious cathodic and anodic peaks are seen in the SS| $\text{Li}_{10}\text{SnP}_2\text{S}_{12}$ |Li-In cell across the voltage range of -0.5 to $5\,\text{V}$, suggesting redox reaction does not happen at the $\text{Li}_{10}\text{SnP}_2\text{S}_{12}$ /Li-In interface [33]. Apart from its superior properties, the price of the raw material for making $\text{Li}_{10}\text{SnP}_2\text{S}_{12}$ is only about 1/3 of $\text{Li}_{10}\text{GeP}_2\text{S}_{12}$ [34]. Moreover, $\text{Li}_{10}\text{SnP}_2\text{S}_{12}$ (LSnPS) has been commercialized under the NANOMYTE brand in powder (SSE-10) and slurry (SSE-10D) was formed [49]. However, the $\text{Li}_{10}\text{SnP}_2\text{S}_{12}$ electrolyte is not stable against the lithium anode [96].

Li₁₀SiP₂S₁₂ (LSiPS) is an alternative electrolyte to substitute Ge in the LGPS electrolytes other than Li₁₀SnP₂S₁₂ (LSnPS). To compare the performance among them, in terms of ionic conductivity, diffusivity, and activation energy values, LSiPS shows a better value than LSnPS. The Li diffusivity of LSiPS was higher than LGPS, while the Li diffusivity of LSnPS was slightly lower. LSiPS has a lower activation energy value than LGPS, while LSnPS has a slightly greater value. Besides, the value of bulk ionic conductivity, when it is compared to LiSnPS, which is derived from NMR diffusivity calculations, LSiPS has a higher value [40]. Li₁₀SiP₂S₁₂ (LSiPS) showed a conductivity value of 2.3×10^{-3} mS cm⁻¹ with 0.29 eV activation energy. This value indicates a high conductivity value for unsintered materials [36]. The combination of Sn and Si to replace Ge resulted in the significant enhancement of ionic conductivity. At ambient temperature, Li₁₀Si_{0.3}Sn_{0.7}P₂S₁₂ have ionic conductivity value of $8 \times 10^{-3} \,\mathrm{S \, cm^{-1}}$, that is relatively high when compared to the materials with single Sn or Si [49]. This shows that the combination of Sn and Si is used in solid-state as an electrolyte material.

Based on the cyclic voltammetry test, the lithium sulfide-based solid electrolyte material shows a wide electrochemical stability window of 0–5 V, including

LGPS [10], LAIPS [87], LSnPS, and LSiPS. However, based on calculations, the electrochemical window of LGPS is narrower than 5 V [97], only in the range of 1.7-2.1 V. Moreover, the stability window value is low compared to other solid electrolyte types, such as LLZO, LATP, and LISICON group [98]. The formation of new interfaces due to the degradation of electrolyte material is the basic problem in solid electrolyte stability. The results reveal that the electrochemical window for both solid electrolytes is substantially narrower than that reported previously based on electrode semiblocking. To overcome the high interfacial resistance, stabilizing the solid electrolyte is required. The key to the good performance of all solid-state Li-ion bulk type batteries is to expand the electrochemical stability window solid electrolyte through spontaneous formation or application of the artificial SEI layer [99] (Table 1).

3 Conclusion and future perspectives

Due to its low cost, strong Li-ion conductivity, and large electrochemical window relative to Li/Li⁺, the binary

(100 - x) Li₂S-xP₂S₅ system, as an important member of solid sulfide electrolytes, is a particularly desirable electrolyte choice for solid-state batteries. Li₃PS₄, Li₇P₃S₁₁, and Li₄P₂S₆ have been extensively studied among various compositions. Li₃PS₄ has good compatibility with lithium metal, Li₇P₃S₁₁ has a high conductivity of greater than 1 mS cm⁻¹ at 298 K, and Li₄P₂S₆ is quite stable in maintaining its structure crystals up to temperatures as high as 950°C in vacuum and up to 280°C in air. Although solid electrolytes based on Li₂S-P₂S₅ come with limitations in terms of chemical and electrochemical stability, they are promising candidates for the next generation of SSBs due to their high ionic conductivity ($>10^{-4}$ S cm⁻¹). To overcome these limitations, the stability of the materials should be assessed in a strict way. Likewise, with the synthesis method used, it is necessary to conduct a thorough examination of the relationship between the synthesis method and the properties of the resulting material.

419

The Li-argyrodite solid electrolyte is another sulfide-based solid electrolyte. At 298 K, argyrodite type solid electrolytes, Li₆PS₅X (X: Cl, Br, and I), have a high ionic conductivity, with values in the range from 10^{-2} to 10^{-3} S cm⁻¹ for Cl and Br. Li₆PS₅X is generally synthesized by the ball milling method, but can also be synthesized by the wet

Table 1: Summary of properties of sulfide solid electrolytes

Sulfide solid electrolytes	lonic conductivity (mS cm ⁻¹)	Activation energy (kJ mol ⁻¹)	Electrochemical stability (V) vs $\mathrm{Li}^+/\mathrm{Li}$	Ref.
Li ₃ PS ₄	0.16	60-73	_	[28,100]
Li ₇ P ₃ S ₁₁	1.3	0.29×10^{-13}	5	[30,49]
$\text{Li}_4\text{P}_2\text{S}_6$	0.002	0.46×10^{-22}	_	[38]
$Li_{10}GeP_2S_{12}$	120	23.156	-0.5 to 5	[10]
$\operatorname{Li}_{10}\operatorname{SnP}_2\operatorname{S}_{12}$	7	26.051	_	[101]
	4	57.89	_	[101]
	2	29.91	_	[102]
	~3	_	0.5 to 5	[103]
	5	25.086	0.5	[104]
	3.2	20.262	-0.5-5	[95]
$Li_{10}SiP_2S_{12}$	2.3	24.025	0-5	[94]
	_	18.332	_	[105]
$Li_{11}AlP_2S_{12}$	0.8	25.086	5	[87]
Li ₆ PS ₅ X	1-10	_	_	[52]
Li ₆ PS ₅ Cl	0.22	25.086	_	[53]
	0.74	10.613	_	[54]
	1.33	28.95-38.59	0-7	[78]
	1.1	15.438	_	[56]
	1.3	30.875	-0.5 to 5 V	[65]
	0.74	_	_	[57]
Li ₆ PS₅Br	1-10	19.3	_	[51]
	0.72	16.403		[54]
	1.38	14.473	0-4.2 V	[55]
	3.1	29.1	_	[66]
Li ₆ PS ₅ I	0.00046	24.121	_	[54]
Li ₄ PS ₄ I	0.12	41.489	_	[75]

chemical method using THF and EtOH as solvents. Apart from its high conductivity, $\text{Li}_6\text{PS}_5\text{X}$ also has the largest chemical stability of any sulfide based solid electrolyte, up to 10~V vs Li/Li^+ . Therefore, with its high electrochemical stability and excellent ionic conductivity value, $\text{Li}_6\text{PS}_5\text{X}$ is acceptable as an SSE in the Li-ion batteries. So, further research to improve the electrochemical performance of $\text{Li}_6\text{PS}_5\text{X}$ still needs to be done to get the best performance from this solid electrolyte.

Based on a review of the types of sulfide-based solid electrolyte that have been carried out, LGPS is a material that has the highest ionic conductivity value. Li₁₀GeP₂S₁₂ (LGPS) has the greatest conductivity value of Li⁺ at room temperature and excellent electrochemical performance. However, the price of Ge required for the synthesis of LGPS is relatively expensive, therefore, it is a big consideration in the use of LGPS as a solid electrolyte. A cheap and abundant source of Ge is needed to reduce the cost. One of the alternative sources is recovering Ge from coal and sphalerites [106]. Ge is an impurity in sphalerites [106]. In addition, recoverable Ge content is also found in coal. The discovery of the Ge content in coal was first made in 1935, when it was known that coal ash contained up to 1.1% Ge [107]. The use of coal in the world is still quite large, reaching 5,400 mtce in 2019 [108]. The estimated ash produced reaches 5% of the amount of coal used. Meanwhile, 75% of the coal ash produced has not been managed properly [109]. This creates opportunities for the utilization of the Ge content in coal ash, in order to reduce the cost of producing LGPS. Besides, the electrochemical stability window of LGPS is quite narrow, 0-5 V or even narrower than that. As a result, increasing the electrochemical stability of this type of solid electrolyte by forming a spontaneous SEI layer or applying an artificial SEI layer is required. Other classes, such as LPS and Li₆PS₅X (X: Cl, Br, and I) are also options for solid electrolyte applications: however, Li_xMP_xS_x (M: Sn, Si, and Al) still outperformed them. Therefore, with its conductivity value, LGPS is the most promising solid electrolyte, but further research is needed to increase the stability window to support perfect electrochemical performance.

Assembling sulfide-based electrolytes in solid-state batteries should be under Ar atmospheric conditions, because of the sensitive nature of the material. The low chemical stability of sulfide-based solid electrolytes to environmental humidity should be overcome. The hydrolysis of solid electrolytes leads to the formation of toxic H_2S gas. The solution offered for the H_2S gas problem is the use of M_xO_y metal oxides, such as Fe_2O_3 , Bi_2O_3 , and ZnO which can act as H_2S gas absorbers, by responding

spontaneously to Gibbs energy from the reaction between M_xO_y and negative H_2S gas to form metal sulfides [88]. This also opens up opportunities for further research on improving the stability of solid electrolyte materials in atmospheric conditions.

Acknowledgment: This article was supported by the Center of Excellence for Electrical Energy Storage, Sebelas Maret University as a provider of facilities and UMG Idealab as a provider of funds for this research.

Conflict of interest: Authors state no conflict of interest.

References

- [1] Liang Y, Zhao C, Yuan H, Chen Y, Zhang W, Huang J, et al. A review of rechargeable batteries for portable electronic devices. InfoMat. 2019;1:1–27.
- [2] Judez X, Martinez-Ibañez M, Santiago A, Armand M, Zhang H, Li C. Quasi-solid-state electrolytes for lithium sulfur batteries: Advances and perspectives. J Power Sources. 2019;438:226985.
- [3] Nishi Y, Power J. Lithium ion secondary batteries; past 10 years and the future. Sources. 2001;100:101-6.
- [4] Li Q, Chen J, Fan L, Kong X, Lu Y. Progress in electrolytes for rechargeable Li-based batteries and beyond. Green Energy Env. 2016;1:18–42.
- [5] Chen Y, Kang Y, Zhao Y, Wang L, Liu J, Li Y, et al. A review of lithium-ion battery safety concerns: The issues, strategies, and testing standards. J Energy Chem. 2021;59:83–99.
- [6] Schmuch R, Wagner R, Hörpel G, Placke T, Winter M. Performance and cost of materials for lithium-based rechargeable automotive batteries. Nat Energy. 2018;3:267–78.
- [7] Janek J, Zeier WG. A solid future for battery development. Nat Energy. 2016;1:1.
- [8] Fan L, Wei S, Li S, Li Q, Lu Y. Recent progress of the solidstate electrolytes for high-energy metal-based batteries. Adv Energy Mater. 2018;8:1–31.
- [9] Gao Z, Sun H, Fu L, Ye F, Zhang Y, Luo W, et al. Promises, challenges, and recent progress of inorganic solid-state electrolytes for all-solid-state lithium batteries. Adv Mater. 2018;30:1–27.
- [10] Kamaya N, Homma K, Yamakawa Y, Hirayama M, Kanno R, Yonemura M, et al. A lithium superionic conductor. Nat Mater. 2011;10:682-6.
- [11] Wang Y, Richards WD, Ong SP, Miara LJ, Kim JC, Mo Y, et al. Design principles for solid-state lithium superionic conductors. Nat Mater. 2015;14:1026-31.
- [12] Sun YK. Promising all-solid-state batteries for future electric vehicles. ACS Energy Lett. 2020;5:3221–3.
- [13] Varzi A, Raccichini R, Passerini S, Scrosati B. Challenges and prospects of the role of solid electrolytes in the revitalization of lithium metal batteries. J Mater Chem A. 2016;4:17251-9.

- [14] Zheng F, Kotobuki M, Song S, Lai MO, Lu L. Review on solid electrolytes for all-solid-state lithium-ion batteries. J Power Sources. 2018;389:198–213.
- [15] Chen MY, Lee KL, Hsu PN, Wu CS, Wu CH. Is there an ethnic difference in the prevalence of lupus cystitis? A report of six cases. Lupus. 2004;167:263–9.
- [16] Xiao T, Xu Z, Zhang H, Geng J, Qiao Y, Liang Y, et al. TP53I11 suppresses epithelial-mesenchymal transition and metastasis of breast cancer cells. Energy Storage Mater. 2019;19:379-84.
- [17] Yan G, Yu S, Nonemacher JF, Tempel H, Kungl H, Malzbender J, et al. Influence of sintering temperature on conductivity and mechanical behavior of the solid electrolyte LATP. Ceram Int. 2019;45:14697–703.
- [18] Aatiq A, Ménétrier M, Croguennec L, Suard E, Delmas C. On the structure of Li₃Ti₂(PO₄)₃. J Mater Chem. 2002;12:2971–8.
- [19] Murugan R, Thangadurai V, Weppner W. Fast lithium ion conduction in garnet-type Li(7)La(3)Zr(2)O(12). Angew Chemie – Int Ed. 2007;46:7778–81.
- [20] Cao S, Song S, Xiang X, Hu Q, Zhang C, Xia Z, et al. Review modeling, preparation, and elemental doping of Li₇La₃Zr₂O₁₂ garnet-type solid electrolytes: A Review. J Korean Ceram Soc. 2019;56:111–29.
- [21] Kato Y, Hori S, Saito T, Suzuki K, Hirayama M, Mitsui A, et al. High-power all-solid-state batteries using sulfide superionic conductors. Nat Energy. 2016;1:1.
- [22] Su QC, Wang X, Deng C, Yun YL, Zhao Y, Peng Y.
 Transcriptome responses to elevated CO₂ level and
 Wolbachia-infection stress in Hylyphantes graminicola
 (Araneae: Linyphiidae). Energy Env Sci. 2020;13:908–20.
- [23] Lau J, DeBlock RH, Butts DM, Ashby DS, Choi CS, Dunn BS. Sulfide solid electrolytes for lithium battery applications. Adv Energy Mater. 2018;8:1.
- [24] Zhang W, Cai L, Cao S, Qiao L, Zeng Y, Zhu Z, et al. Electrode materials: interfacial lattice-strain-driven generation of oxygen vacancies in an aerobic-annealed TiO₂(B) Electrode (Adv. Mater. 52/2019). Adv Mater. 2019;31:1.
- [25] Chen S, Xie D, Liu G, Mwizerwa JP, Zhang Q, Zhao Y, et al. Sulfide solid electrolytes for all-solid-state lithium batteries: Structure, conductivity, stability and application. Energy Storage Mater. 2018;14:58–74.
- [26] Dietrich C, Weber DA, Sedlmaier SJ, Indris S, Culver SP, Walter D, et al. Lithium ion conductivity in Li₂S-P₂S₅ glasses – building units and local structure evolution during the crystallization of superionic conductors Li₃PS₄, Li₇P₃S₁₁and Li₄P₂S₇. J Mater Chem A. 2017;5:18111-9.
- [27] Homma K, Yonemura M, Nagao M, Hirayama M, Kanno R. Crystal structure of high-temperature phase of lithium ionic conductor, Li₃PS₄. Journal of the Physical Society of Japan. 2010;79:90–3.
- [28] Liu Z, Fu W, Payzant EA, Yu X, Wu Z, Dudney NJ, et al. Anomalous high ionic conductivity of nanoporous β-Li₃PS₄. J Am Chem Soc. 2013;135:975–8.
- [29] Phuc NHH, Morikawa K, Totani M, Muto H, Matsuda A. Chemical synthesis of Li₃PS₄ precursor suspension by liquidphase shaking. Solid State Ion. 2016;285:2–5.
- [30] Chu IH, Nguyen H, Hy S, Lin YC, Wang Z, Xu Z, et al. Insights into the Performance Limits of the Li₇P₃S₁₁ Superionic Conductor: A Combined First-Principles and Experimental Study. ACS Appl Mater Interfaces. 2016;8:7843–53.

- [31] Yamane H, Shibata M, Shimane Y, Junke T, Seino Y, Adams S, et al. Crystal structure of a superionic conductor, Li₇P₃S₁₁. Solid State Ion. 2007;178:1163-7.
- [32] Minami K, Mizuno F, Hayashi A, Tatsumisago M. Lithium ion conductivity of the Li₂S-P₂S₅ glass-based electrolytes prepared by the melt quenching method. Solid State Ion. 2007;178:837-41.
- [33] Minami K, Hayashi A, Tatsumisago M. Preparation and characterization of superionic conducting Li₇P₃S₁₁ crystal from glassy liquids. J Ceram Soc Jpn. 2010;118:305–8.
- [34] Hayashi A, Minami K, Tatsumisago M. Development of sulfide glass-ceramic electrolytes for all-solid-state lithium rechargeable batteries. J Solid State Electrochem. 2010:14:1761-7.
- [35] Mercier R, Malugani JP, Fahys B, Robert G, Douglade J. Structure du tetrathiophosphate de lithium. Acta Crystallogr Sect B Struct Crystallogr Cryst Chem. 1982;38:1887-90.
- [36] Hood ZD, Kates C, Kirkham M, Adhikari S, Liang C, Holzwarth N. Structural and electrolyte properties of Li₄P₂S₆. Solid State Ion. 2016;284:61-70.
- [37] Tatsumisago M, Hayashi A. Preparation of lithium ion conducting glasses and glass-ceramics for all-solid-state batteries. J Non Cryst Solids. 2008;354:1411-7.
- [38] Mizuno F, Hayashi A, Tadanaga K, Tatsumisago M. High lithium ion conducting glass-ceramics in the system Li₂S-P₂S₅. Solid State Ion. 2006;177:2721-5.
- [39] Homma K, Yonemura M, Kobayashi T, Nagao M, Hirayama M, Kanno R. Crystal structure and phase transitions of the lithium ionic conductor Li₃PS₄. Solid State Ion. 2011;182:53–8.
- [40] Mercier R, Malugani JP, Fahys B, Douglande J, Robert G. Synthese, structure cristalline et analyse vibrationnelle de l'hexathiohypodiphosphate de lithium Li₄P₂S₆. J Solid State Chem. 1982;43:151–62.
- [41] Kudu ÖU, Famprikis T, Fleutot B, Braida MD, Le Mercier T, Islam MS, et al. A review of structural properties and synthesis methods of solid electrolyte materials in the $\text{Li}_2\text{S} \text{P}_2\text{S}_5$ binary system. J Power Sources. 2018;407:31–43.
- [42] Dietrich C, Sadowski M, Sicolo S, Weber DA, Sedlmaier SJ, Weldert KS, et al. Local Structural Investigations, Defect Formation, and Ionic Conductivity of the Lithium Ionic Conductor Li₄P₂S₆. Chem Mater. 2016;28:8764–73.
- [43] Liang J, Li X, Zhao Y, Goncharova LV, Wang G, Adair KR, et al. In situ Li3PS4 solid-state electrolyte protection layers for superior long-life and high-rate lithium-metal anodes. Adv Mater. 2018;30:1–9.
- [44] Tsukasaki H, Mori S, Shiotani S, Yamamura H. Ionic conductivity and crystallization process in the Li₂S-P₂S₅ glass electrolyte. Solid State Ion. 2018;317:122-6.
- [45] Tachez M, Malugani J, Mercier R, Robert G. Ionic conductivity of and phase transition in lithium thiophosphate Li₃PS₄. Solid State Ion. 1984;14:181-5.
- [46] Aoki Y, Ogawa K, Nakagawa T, Hasegawa Y, Sakiyama Y, Kojima T, et al. Chemical and structural changes of 70Li₂S-30P₂S₅ solid electrolyte during heat treatment. Solid State Ion. 2017;310:50-5.
- [47] Hayashi A, Hama S, Minami T, Tatsumisago M. Formation of superionic crystals from mechanically milled Li₂S-P₂S₅ glasses. Electrochem Commun. 2003;5:111-4.

- [48] Khurram Tufail M, Ahmad N, Zhou L, Faheem M, Yang L, Chen R, et al. Insight on air-induced degradation mechanism of Li₇P₃S₁₁ to design a chemical-stable solid electrolyte with high Li₂S utilization in all-solid-state Li/S batteries. Chem Eng J. 2021;425:130535.
- Wenzel S, Weber DA, Leichtweiss T, Busche MR, Sann J, Janek J. Interphase formation and degradation of charge transfer kinetics between a lithium metal anode and highly crystalline $Li_7P_3S_{11}$ solid electrolyte. Solid State Ion. 2016;286:24-33.
- Liu Y, Yang Y. Recent progress of TiO2-based anodes for Li ion batteries. J Nanomater. 2016;2:1-15.
- Epp V, Gün Ö, Deiseroth HJ, Wilkening M. Highly Mobile Ions: Low-Temperature NMR Directly Probes Extremely Fast Li+Hopping in Argyrodite-Type Li₆PS₅Br. J Phys Chem Lett. 2013;4:2118-23.
- Deiseroth H-J, Kong ST, Eckert H, Vannahme J, Reiner C, [52] Zaiß T, et al. Li₆PS₅X: A Class of Crystalline Li-Rich Solids With an Unusually High Li⁺ Mobility. Angew Chem. 2008;120:767-70.
- Rao RP, Adams S. Studies of lithium argyrodite solid elec-[53] trolytes for all-solid-state batteries. Phys Status Solidi A. 2011:208:1804-7.
- [54] Rayavarapu PR, Sharma N, Peterson VK, Adams S. Variation in structure and Li⁺-ion migration in argyrodite-type Li₆PS₅X (X = Cl, Br, I) solid electrolytes. J Solid State Electrochem. 2012;16:1807-13.
- Yu S, Siegel DJ, Yu L, Grace T, Batmunkh M, Dadkhah M, et al. [55] Grain Boundary Contributions to Li-Ion Transport in the Solid Electrolyte $Li_7La_3Zr_2O_{12}(LLZO.$ J Mater Chem A. 2017;29:9639-47.
- Rao RP, Sharma N, Peterson VK, Adams S. Formation and conductivity studies of lithium argyrodite solid electrolytes using in-situ neutron diffraction. Solid State Ion. 2013;230:72-6.
- Zhou L, Park KH, Sun X, Lalère F, Adermann T, Hartmann P, et al. Solvent-Engineered Design of Argyrodite Li₆PS₅X (X = Cl, Br, I) Solid Electrolytes with High Ionic Conductivity. ACS Energy Lett. 2019;4:265-70.
- [58] Duan H, Zheng H, Zhou Y, Xu B, Liu H. Stability of garnet-type Li ion conductors: An overview. Solid State Ion. 2018;318:45-53.
- Reddy MV, Julien CM, Mauger A, Zaghib K. Sulfide and Oxide Inorganic Solid Electrolytes for All-Solid-State Li Batteries: A Review. Nanomaterials. 2020;10:1.
- Gautam A, Ghidiu M, Suard E, Kraft MA, Zeier WG. On the Lithium Distribution in Halide Superionic Argyrodites by Halide Incorporation in Li₇-xPS₆-xClx. ACS Appl Energy Mater. 2021;4:7309-15.
- [61] Bai X, Duan Y, Zhuang W, Yang R, Wang J. Research progress in Li-argyrodite-based solid-state electrolytes. J Mater Chem A. 2020;8:25663-86.
- Hanghofer I, Gadermaier B, Wilkening HMR. Fast Rotational [62] Dynamics in Argyrodite-Type Li_6PS_5X (X: Cl, Br, I) as Seen by31P Nuclear Magnetic Relaxation—On Cation-Anion Coupled Transport in Thiophosphates. Chem Mater. 2019:31:4591-7.
- Arnold W, Buchberger DA, Li Y, Sunkara M, Druffel T, Wang H. Halide doping effect on solvent-synthesized lithium

- argyrodites Li₆PS₅X (X= Cl, Br, I) superionic conductors. J Power Sources. 2020;464:1.
- Xu J, Liu L, Yao N, Wu F, Li H, Chen L. Liquid-involved synth-[64] esis and processing of sulfide-based solid electrolytes, electrodes, and all-solid-state batteries. Mater Today Nano. 2019;8:100048.
- Zhang J, Zhong H, Zheng C, Xia Y, Liang C, Huang H, et al. All-[65] solid-state batteries with slurry coated LiNi_{0.8}Co_{0.1}Mn_{0.1}O₂ composite cathode and Li₆PS₅Cl electrolyte: Effect of binder content. J Power Sources. 2018;391:73-9.
- [66] Yubuchi S, Uematsu M, Hotehama C, Sakuda A, Hayashi A, Tatsumisago M. An argyrodite sulfide-based superionic conductor synthesized by a liquid-phase technique with tetrahydrofuran and ethanol. I Mater Chem A. 2019;7:558-66.
- Minafra N, Culver SP, Krauskopf T, Senyshyn A, Zeier WG. [67] Effect of Si substitution on the structural and transport properties of superionic Li-argyrodites. J Mater Chem A. 2018;6:645-51.
- [68] Bernges T, Culver SP, Minafra N, Koerver R, Zeier WG. Competing Structural Influences in the Li Superionic Conducting Argyrodites $Li_6PS_{5^-}$ xSe xBr $(0 \le x \le 1)$ upon Se Substitution. Inorg Chem. 2018;57:13920-8.
- [69] Chen M, Yin X, Reddy MV, Adams S. All-solid-state MoS₂/ Li₆PS₅Br/In-Li batteries as a novel type of Li/S battery. J Mater Chem A. 2015;3:10698-702.
- [70] Chen M, Adams S. High performance all-solid-state lithium/ sulfur batteries using lithium argyrodite electrolyte. J Solid State Electrochem. 2015;19:697-702.
- [71] Chen M, Rao RP, Adams S. High capacity all-solid-state Cu-Li₂S/Li₆PS₅Br/In batteries. Solid State Ion. 2014;262:183-7.
- [72] Chen M, Prasada R, Rao S, Adams S. The unusual role of Li₆PS₅Br in all-solid-state CuS/Li₆PS₅Br/In-Li batteries. Solid State Ion. 2014;268:300-4.
- [73] Rangasamy E, Liu Z, Gobet M, Pilar K, Sahu G, Zhou W, et al. An iodide-based Li₇P₂S₈I superionic conductor. J Am Chem Soc. 2015;137:1384-7.
- [74] Pecher O, Kong ST, Goebel T, Nickel V, Weichert K, Reiner C, et al. Atomistic characterisation of Li+ mobility and conductivity in Li(7-x)PS(6-x)Ix argyrodites from molecular dynamics simulations, solid-state NMR, and impedance spectroscopy. Chem - A Eur J. 2010;16:8347-54.
- Sedlmaier SJ, Indris S, Dietrich C, Yavuz M, Dräger C, von [75] Seggern F, et al. Li₄PS₄I: A Li⁺ superionic conductor synthesized by a solvent-based soft chemistry approach. Chem Mater. 2017;29:1830-5.
- [76] Kraft MA, Ohno S, Zinkevich T, Koerver R, Culver SP, Fuchs T, et al. Inducing high ionic conductivity in the lithium superionic argyrodites li₆+ xp1- xge xs5i for all-solid-state batteries. J Am Chem Soc. 2018;140:16330-9.
- Ma Z, Xue HG, Guo SP. Recent achievements on sulfide-type [77] solid electrolytes: crystal structures and electrochemical performance. J Mater Sci. 2018;53:3927-38.
- [78] Boulineau S, Courty M, Tarascon JM, Viallet V. Mechanochemical synthesis of Li-argyrodite Li₆PS₅X (X=Cl, Br, I) as sulfur-based solid electrolytes for all solid state batteries application. Solid State Ion. 2012;221:1-5.

- [79] Takada K, Power J. Progress in solid electrolytes toward realizing solid-state lithium batteries. Sources. 2018;394:74–85.
- [80] Ohta S, Kobayashi T, Asaoka T. High lithium ionic conductivity in the garnet-type oxide $Li_{7-x}La_3(Zr_{2-x},Nb_x)O_{12}$ (X = 0-2). J Power Sources. 2011;196:3342-5.
- [81] Deiseroth HJ, Maier J, Weichert K, Nickel V, Kong ST, Reiner C. Li7PS6 and Li6PS5X (X: Cl, Br, I): possible three-dimensional diffusion pathways for lithium ions and temperature dependence of the ionic conductivity by impedance measurements. Z Fur Anorg Und Allg Chem. 2011;637:1287–94.
- [82] Kato Y, Kawamoto K, Kanno R, Hirayama M. Discharge performance of all-solid-state battery using a lithium superionic conductor Li₁₀GeP₂S₁₂. Electrochemistry. 2012;80:749-51.
- [83] Lee YG, Fujiki S, Jung C, Suzuki N, Yashiro N, Omoda R, et al. High-energy long-cycling all-solid-state lithium metal batteries enabled by silver-carbon composite anodes. Nat Energy. 2020;5:299-308.
- [84] Suh KS, Hojjaji A, Villenueve G, Ménétrier M, Levasseur A. ¹¹B NMR studies of the local environment of boron in B2S3-Li2S-LiI glasses. J Non Cryst Solids. 1991;128:13-7.
- [85] Tsukasaki H, Otoyama M, Mori Y, Mori S, Morimoto H, Hayashi A, et al. Analysis of structural and thermal stability in the positive electrode for sulfide-based all-solid-state lithium batteries. J Power Sources. 2017;367:42-8.
- [86] Zhao Y, Wu C, Peng G, Chen X, Yao X, Bai Y, et al. A new solid polymer electrolyte incorporating $\text{Li}_{10}\text{GeP}_2\text{S}_{12}$ into a polyethylene oxide matrix for all-solid-state lithium batteries. J Power Sources. 2016;301:47–53.
- [87] Zhou P, Wang J, Cheng F, Li F, Chen J. A solid lithium superionic conductor Li₁₁AlP₂S₁₂ with a thio-LISICON analogous structure. Chem Commun. 2016;52:6091–4.
- [88] Ohtomo T, Hayashi A, Tatsumisago M, Kawamoto K. Suppression of H_2S gas generation from the $75Li_2S\cdot25P_2S_5$ glass electrolyte by additives. J Mater Sci. 2013;48:4137–42.
- [89] Kwon O, Hirayama M, Suzuki K, Kato Y, Saito T, Yonemura M, et al. Synthesis, structure, and conduction mechanism of the lithium superionic conductor Li₁₀+δGe₁+δP₂–δS₁₂. J Mater Chem A. 2015;3:438–46.
- [90] Weber DA, Senyshyn A, Weldert KS, Wenzel S, Zhang W, Kaiser R, et al. Structural Insights and 3D Diffusion Pathways within the Lithium Superionic Conductor Li₁₀GeP₂S₁₂. Chem Mater. 2016;28:5905–15.
- [91] Hassoun J, Verrelli R, Reale P, Panero S, Mariotto G, Greenbaum S, et al. A structural, spectroscopic and electrochemical study of a lithium ion conducting Li₁₀GeP₂S₁₂ solid electrolyte. J Power Sources. 2013;229:117–22.
- [92] Yin J, Yao X, Peng G, Yang J, Huang Z, Liu D, et al. Influence of the Li-Ge-P-S based solid electrolytes on NCA electrochemical performances in all-solid-state lithium batteries. Solid State Ion. 2015;274:8-11.

- [93] Kanno R, Murayama M. Lithium ionic conductor thio-LISICON: the Li₂SGeS₂P₂S₅ system. J Electrochem Soc. 2001;148:A742-6.
- [94] Whiteley JM, Woo JH, Hu E, Nam KW, Lee SH. Empowering the Lithium Metal Battery through a Silicon-Based Superionic Conductor. J Electrochem Soc. 2014;161:A1812-7.
- [95] Yi J, Chen L, Liu Y, Geng H, Fan LZ. High capacity and superior cyclic performances of all-solid-state lithium-sulfur batteries enabled by high-conductivity Li₁₀SnP₂S₁₂ solid electrolyte. ACS Appl Mater Interfaces. 2019;1:36674–81.
- [96] Rettenwander D, Wagner R, Reyer A, Bonta M, Cheng L, Doeff MM, et al. Interface Instability of Fe-Stabilized Li₇La₃Zr₂O₁₂ versus Li Metal. J Phys Chem. 2018:122:3780–5.
- [97] Mo Y, Ong SP, Ceder G. First principles study of the Li₁₀GeP₂S₁₂ lithium super ionic conductor material. Chem Mater. 2012;24:15–7.
- [98] Binninger T, Marcolongo A, Mottet M, Weber V, Laino T. Comparison of computational methods for the electrochemical stability window of solid-state electrolyte materials. J Mater Chem A. 2020;8:1347-59.
- [99] Han F, Zhu Y, He X, Mo Y, Wang C. Electrochemical stability of Li₁₀GeP₂S₁₂ and Li₇La₃Zr₂O₁₂ solid electrolytes. Adv Energy Mater. 2016;6:1–9.
- [100] Iikubo S, Shimoyama K, Kawano S, Fujii M, Yamamoto K, Matsushita M, et al. Novel stable structure of Li₃PS₄ predicted by evolutionary algorithm under high-pressure. AIP Adv. 2018;8:015008.
- [101] Bron P, Johansson S, Zick K, Gunne JS, Dehnen S, Rolling B. Li₁₀SnP₂S₁₂: An affordable lithium superionic conductor. J Am Chem Soc. 2013;135:15694–7.
- [102] Bron P, Dehnen S, Roling B. Li₁₀Si_{0.3}Sn_{0.7}P₂S₁₂ A low-cost and low-grain-boundary-resistance lithium superionic conductor. J Power Sources. 2016;329:530–5.
- [103] Vinado C, Wang S, He Y, Xiao X, Li Y, Wang C, et al. Electrochemical and interfacial behavior of all solid state batteries using $\text{Li}_{10}\text{SnP}_2\text{S}_{12}$ solid electrolyte. J Power Sources. 2018;396:824–30.
- [104] Tarhouchi I, Viallet V, Vinatier P, Ménétrier M. Electrochemical characterization of Li₁₀SnP₂S₁₂: An electrolyte or a negative electrode for solid state Li-ion batteries. Solid State Ion. 2016;296:18–25.
- [105] Kuhn A, Gerbig O, Zhu C, Falkenberg F, Maier J, Lotsch BV. A new ultrafast superionic Li-conductor: ion dynamics in Li₁₁Si₂PS₁₂ and comparison with other tetragonal LGPS-type electrolytes. Phys Chem Chem Phys. 2014;16:14669-74.
- [106] Frenzel M, Ketris MP, Gutzmer J. On the geological availability of germanium. Min Depos. 2014;49:471–86.
- [107] Goldschmidt VM. Rare Elements in Coal Ashes. Ind Eng Chem. 1935;27:1100-2.
- [108] Prime J, Martinez LM. Statistucs report coal information Overview. Paris; 2020.
- [109] Sommerville R, Blissett R, Rowson N, Blackburn S. Producing a Synthetic Zeolite from Improved Fly Ash Residue. Int J Min Process. 2013;124:20–5.